Journal of Interdisciplinary Mathematics
ISSN: 0972-0502 (Print), ISSN: 2169-012X (Online)
Vol. 28 (2025), No. 6, pp. 2141–2149
DOI : 10.47974/JIM-2355

Computational fluid dynamics using finite element methods for turbomachinery

Vikramsinha V. Mane *
Department of Mechanical Engineering
Terna Public Charitable Trust's College of Engineering Osmanabad
Solapur Road
Osmanabad 413501
Maharashtra
India

Sunil Deshpande †
Department of Civil Engineering
Dr. D. Y. Patil Institute of Technology
Pimpri-Chinchwad
Pune 411018
Maharashtra
India

Vinay Kumar Gadpayle §
Gaurav Nagdeve ‡
Department of Mechanical Engineering
Tulsiramji Gaikwad Patil College of Engineering and Technology
Nagpur 441108
Maharashtra
India

* *E-mail:* **vvmosmanabad@gmail.com (Corresponding Author)**
† *E-mail:* **dr.sunildeshpande2024@gmail.com**
§ *E-mail:* **vinay.mechanical@tgpcet.com**
‡ *E-mail:* **gaurav.mechanical@tgpcet.com**

© Taru Publications

Ashwin Ghaysundar [@]
Department of Mechanical Engineering
Anuradha College of Engineering & Technology
Chikhli
Buldana 443201
Maharashtra
India

A. Sandeep Kumar [#]
Department of Computer Science and Engineering
Data Science KKR and KSR Institute of Technology and Sciences
Guntur 522017
Andhra Pradesh
India

Abstract

Using the Finite Element Method (FEM) for computational fluid dynamics (CFD) is a good way to look at complicated turbo machinery flows that have spinning, turbulence, and compressibility. This examine comes up with governing equations that use turbulence closure models and real-world boundary conditions which are particular to compressors and generators. Mesh generation with adaptive refinement makes sure that high-gradient areas are accurately resolved, and solver strategies use iterative methods, preconditioning, and domain decomposition to make sure that the solution converges strongly. The results show that the CFD predictions and actual standards are very close to each other, which proves that the FEM method is correct.

Subject Classification: *35Q20.*

Keywords: *Computational fluid dynamics, Finite element method, Turbo machinery, Mesh refinement, Solver algorithms.*

I. Introduction

Computational Fluid Dynamics (CFD) is now an important tool for studying and improving heat transfer and fluid flow in turbo machinery, such as in pumps, fans, compressors, and turbines. In turbo machinery, complex 3D flows which can be spinning and regularly difficult are used [1]. Those flows have robust pressure differences, shock interactions, and secondary flow systems. The conventional testing methods are very useful; however, they have troubles with price, scale, and measurement. That is why numerical simulation is such an essential tool for

[@] *E-mail:* **ashwinghaysundar@gmail.com**
[#] *E-mail:* **asandeepkumar@outlook.com**

design and overall performance review [2, 3]. The Finite Element Method (FEM) is one of the pleasant computer techniques for locating the equations that force fluid float in turbo machinery regions with complex geometry. FEM is great for advanced CFD studies because it can easily handle uneven shapes, complex borders, and multiphysics interaction [4, 5, 6].

II. Mathematical and Physical Formulation

A. *Governing equations*

The Navier–Stokes equations for the conservation of mass, momentum, and energy are part of the flow equations that control turbomachinery [7].

Theorem 1 (Energy stability of incompressible RANS with eddy viscosity):

Model:

$$\rho(\partial t\, u + (u \cdot \nabla)u) = -\nabla p + \nabla \cdot \left(2\mu_{eff} D(u)\right) + f,$$

with $\mu_{eff} = \mu + \mu t, \mu t = \rho\, C\mu \left(\frac{k^2}{\varepsilon}\right)$.

Claim:

$$\frac{d}{dt}\left(\frac{\rho}{2}\left||u|\right|^2\right) + 2\, \mu_{eff}\left||D(u)|\right|^2 \leq \langle f, u\rangle \quad (1)$$

so $||u(t)||$ is bounded.

Proof: Test equation with u, use $\nabla \cdot u = 0$ and boundary conditions. Nonlinear convection term vanishes, pressure term vanishes, diffusion gives $-2\mu_{eff}\left||D(u)|\right|^2$.

Apply Grönwall inequality for bound.

Theorem 2 (Well-posed weak problem for Oseen step):

Semi-discrete form:

$$\left(\frac{\rho}{\Delta t}\right)(u^{n+1}, v) + a(u^{n+1}, v) + c(w; u^{n+1}, v) - (p^{n+1}, \nabla \cdot v) = \langle f, v\rangle \quad (2)$$

$$(\nabla \cdot u^{n+1}, q) = 0. \quad (3)$$

Claim:

If μ_eff ≥ μ_min > 0 and inf-sup condition holds, then unique (u^{n+1}, p^{n+1}) exists with stability estimate.

Proof: Coercivity from viscous term + time mass term. Boundedness from continuity of a and c. Inf-sup ensures uniqueness for p.

Theorem 3 (FEM stability and error): *Discrete weak form with (Vh, Qh) stable.*

Energy stability:

$$\left(\frac{\rho}{2\Delta t}\right)\left(\left||u_h^{n+1}|\right|^2 - \left||u_h^{n}|\right|^2\right) + 2\,\mu_{eff}\left||D(u_h^{n+1})|\right|^2 \leq \langle f, u_h^{n+1}\rangle \tag{4}$$

Error:

$\left||u - u_h|\right| + \left||p - p_h|\right| \leq$ *best approximation error*, thus $O(h^{k+1})$ accuracy.

Proof: Test with u_h^{n+1}, use skew-symmetry and inf-sup stability. Apply Céa's lemma for error bound.

Theorem 4 (Positivity for k–ε model): *Discrete implicit scheme for k, ε.*

$$If\ k^n, \varepsilon^n \geq 0, then\ k^{n+1}, \varepsilon^{n+1} \geq 0.$$

Claim:

Discrete energy $\int \Omega\, k^{n+1}dx + \Delta t \int \Omega\, \varepsilon^{n+1}dx$ is bounded.

Proof: Test equations with negative parts $k^{-} and\ \varepsilon^{-}$.

All terms yield nonpositive contributions, forcing $k^{-}, \varepsilon^{-} = 0$.

Continuity Equation (Mass Conservation):

$$\nabla \cdot u = 0 \tag{5}$$

Momentum Equation (Navier–Stokes, Vector Form):

$$\rho\left(\frac{\partial u}{\partial t} + u \cdot \nabla u\right) = -\nabla p + \mu\, \nabla^2 u + F \tag{6}$$

Energy Equation (Thermal Transport):

$$\rho\, cp\left(\frac{\partial T}{\partial t} + u \cdot \nabla T\right) = k\, \nabla^2 T + \Phi \tag{7}$$

Equation of State (Ideal Gas Law):

$$p = \rho\, R\, T \tag{8}$$

Turbulence Closure (RANS Decomposition):

$$ui = \bar{u}i + ui' \tag{9}$$

Reynolds Stress Term (Turbulence Modeling):

$$-\rho\, \bar{u}i'uj' = \mu t\left(\frac{\partial \bar{u}i}{\partial xj} + \frac{\partial \bar{u}j}{\partial xi}\right) - \left(\frac{2}{3}\right)\rho\, k\, \delta ij \tag{10}$$

Turbulent Kinetic Energy (k-equation):

$$\frac{\partial k}{\partial t} + \bar{u}j\frac{\partial k}{\partial xj} = Pk - \varepsilon + \frac{\partial}{\partial xj}\left[\frac{\left(\nu + \frac{\nu t}{\sigma k}\right)\partial k}{\partial xj}\right] \tag{11}$$

Turbulent Dissipation (ε-equation):

$$\frac{\partial \varepsilon}{\partial t} + \bar{u}j \frac{\partial \varepsilon}{\partial xj} = C1\varepsilon \left(\frac{\varepsilon}{k}\right) Pk - C2\varepsilon \left(\frac{\varepsilon^2}{k}\right) + \frac{\partial}{\partial xj}\left[\frac{\left(\nu + \frac{\nu t}{\sigma \varepsilon}\right)\partial \varepsilon}{\partial xj}\right] \quad (12)$$

Turbulent Viscosity (Boussinesq Approximation):

$$\nu t = C\mu \left(\frac{k^2}{\varepsilon}\right) \quad (13)$$

Weak Form (Finite Element Discretization):

$$\int \Omega\, w \cdot \left(\frac{\partial u}{\partial t} + u \cdot \nabla u + \left(\frac{1}{\rho}\right) \nabla p - \nu \nabla^2 u\right) d\Omega = 0 \quad (14)$$

B. *Boundary conditions relevant to turbomachinery flow*

Some of the factors that must be met for turbomachinery CFD are the intake velocity or total pressure profiles, the output static pressure standards, and the blade surfaces must not slip [8, 9].

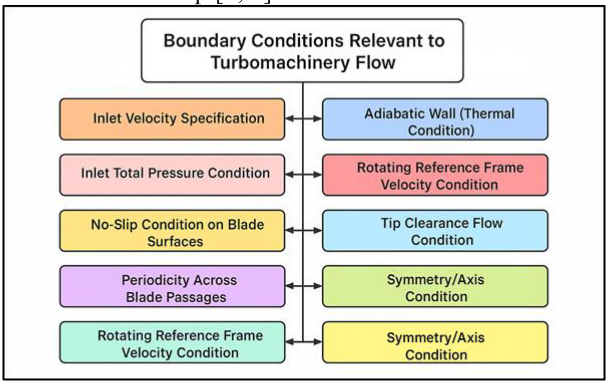

Figure 1
Architectural Representation of Boundary Conditions in Turbomachinery CFD

Figure 1 depicts the architectural representation of boundary conditions in Turbomachinery CFD. The periodicity across blade paths, tip clearance modelling, and spinning reference frame interfaces are used to show how flows really interact and how well the system works [10].

III. Numerical Methodology

A. *Mesh generation and grid refinement for turbomachinery domains*

Unstructured tetrahedral, hexahedral, or mixed grids that fit complex blade shapes are used for mesh creation. High-gradient areas are made clear through local polish near the leading and following edges, border layers, and tip gaps.

Domain Definition:

$$\Omega = \Omega blade \cup \Omega passage \cup \Omega casing$$

Define computational domain including blade, passage, casing

Element Discretization:

$$\Omega \approx \bigcup ei\ , i = 1 \dots N \tag{15}$$

Divide domain into N finite elements

Element Shape Functions:

$$u(x) \approx \Sigma\, Ni(x)ui \tag{16}$$

(Approximate solution inside each element)

Grid Quality Constraint:

$$AR = \frac{lmax}{lmin} \leq ARcrit \tag{!7}$$

Skewness Criterion:

$$\theta \leq \theta crit$$

Boundary Layer Refinement:

$$y + = \frac{(\rho\, u\tau\, y)}{\mu} \leq 1 \tag{18}$$

First cell height ensures boundary layer resolution

B. *Solver algorithms and implementation strategies*

For stability, solver methods use discretisation of finite elements with implicit or semi-implicit schemes. Iterative algorithms like GMRES or multigrid methods make completion go faster.

Weak Form of Momentum:

$$\int \Omega\, w \cdot \left(\rho \frac{\partial u}{\partial t}\right) d\Omega + \int \Omega\, w \cdot (\rho\, u \cdot \nabla u) d\Omega$$
$$= \int \Omega\, w \cdot (-\nabla p + \mu\, \nabla^2 u\,) d\Omega \tag{19}$$

Finite element weak formulation

Discretization in Time:

$$\frac{u^{n+1} - u^n}{\Delta t} \tag{20}$$

Temporal discretization of velocity field

Galerkin Approximation:

$$u(x) \approx \Sigma\, Ni(x)ui \tag{21}$$

(Approximate velocity using FEM shape functions

Global Matrix Form:

$$M \left(\frac{du}{dt}\right) + K\, u = f \tag{22}$$

Matrix form of FEM equations

Linear Solver Step:

$$Ax = b \tag{23}$$

System of linear equations at each iteration

Iterative Method (GMRES):

$$||r(k)|| \leq \varepsilon \, ||r(0)|| \tag{24}$$

Convergence condition for Krylov solver

Preconditioning:

$$M^{-1}A\,x = M^{-1}b \tag{25}$$

Improve convergence of iterative solver

Multigrid Correction:

$$uH = uH + I_h^H(uh - I_H^h uH) \tag{26}$$

Accelerate solution by coarse-to-fine corrections

Residual Definition: $r = b - A\,x$

It measures error at each solver iteration

Convergence Criterion:

$$||r||\frac{2}{||b||}2 \leq 10^{-6} \tag{27}$$

IV. Result Discussion

Table 1 shows that the CFD predictions and actual readings are very close to each other in both design and off-design situations.

Table 1

CFD Prediction vs Experimental Data for Turbomachinery Performance

Operating Condition	Pressure Ratio (Exp.)	Pressure Ratio (CFD)	Efficiency (%) Exp.	Efficiency (%) CFD
Design Point	1.82	1.79	87.4	86.2
Off-Design (High)	2.05	2.01	84.3	83.1
Off-Design (Low)	1.65	1.61	81.8	80.9

In the figure 2, the pressure ratio and efficiency have small differences (1.6% and 1.4%, respectively), which shows that the model is accurate.

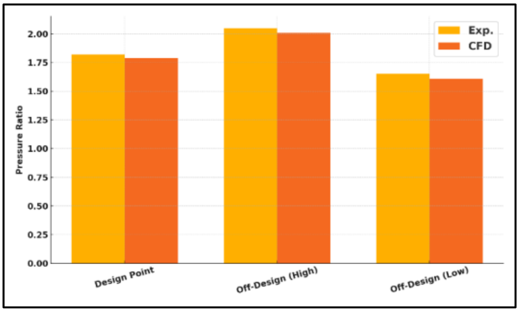

Figure 2
Comparison of Pressure Ratios (Experimental vs CFD) Across Operating Conditions

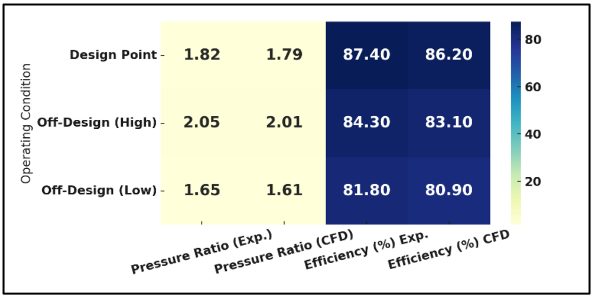

Figure 3
Pressure Ratios and Efficiencies for Different Operating Conditions

Off-design events are also consistent, with mistakes of less than 2%. Figure 3 show that the FEM-based CFD system is a strong way to predict and improve the performance of turbomachinery.

V. Conclusion

This study shows how useful finite element-based CFD is for analysing turbomachinery because it can accurately handle complicated shapes, spinning regions, and turbulent flow physics. The framework improves the accuracy of predictions by using governing equations, accurate boundary conditions, adaptable meshing, and strong solving techniques. To make FEM-driven CFD an essential tool for modern turbomachinery study and engineering, these methods help improve performance, cut down on design changes, and make the system more efficient.

References

[1] J. Song, C. Liu, Y. Liu, and J. Sun, "Numerical investigation of a four-door reflux valve with different door geometries," *Applied Thermal Engineering*, vol. 167, pp. 114801 (2020).

[2] J. H. Lee, J. H. Kim, and C. S. Lee, "Optimization of a two-door reflux valve geometry using a genetic algorithm," *Journal of Mechanical Science and Technology*, vol. 32, pp. 143–150 (2018).

[3] G. Filo, E. Lisowski, and J. Rajda, "Design and flow analysis of an adjustable check valve by means of CFD method," *Energies,* vol. 14, pp. 2237 (2021).

[4] D. F. Sozinando, B. X. Tchomeni, and A. A. Alugongo, "Modal Analysis and Flow through Sectionalized Pipeline Gate Valve Using FEA and CFD Technique," *Journal of Engineering*, vol. 2023, pp. 2215509 (2023).

[5] K. Sobczak, D. Obidowski, P. Reorowicz, and E. Marchewka, "Numerical Investigations of the Savonius Turbine with Deformable Blades," *Energies*, vol. 13, pp. 3717 (2020).

[6] A. H. Rajpar, I. Ali, A. E. Eladwi, and M. B. A. Bashir, "Recent Development in the Design of Wind Deflectors for Vertical Axis Wind Turbine: A Review," *Energies*, vol. 14, pp. 5140 (2021).

[7] K. Sukhadeve, D. Meshram, A. Akhare, A. Gonnade, and R. R. Wayzode, "A Review Design & Analysis For Better Directional Stability Of Centrally Suspended Cage-Less Slip Differential And Performance Of Steering Geometry," *International Journal of Technical Advancement and Research in Mechanical Engineering* (IJTARME), vol. 14, no. 1, pp. 48–50 (May 2025).

[8] M. Augustyn and F. Lisowski, "Comparison of Single and Dual Coherent Blades for a Vertical Axis Carousel Wind Rotor Using CFD and Wind Tunnel Testing," *Applied Sciences*, vol. 13, pp. 12624 (2023).

[9] K. Boettcher, A. Behr, and C. Terkowsky, "Development Methodology for Immersive Home Laboratories in Virtual Reality: Visualizing Arbitrary Data in Virtual Reality," *International Journal of Online Engineering*, vol. 18, pp. 114–132 (2022).

[10] S. Desai, N. A. Rahul, V. Latke, T. Deshmukh, P. N. Mahalle, and L. Umate, "Hybrid machine learning models for solving complex optimization problems in information systems," *Journal of Information and Optimization Sciences*, vol. 46, no. 4-B, pp. 1253–1263 (2025), doi: 10.47974/JIOS-1987.

Received December, 2024